

Communication

# Physical, Deformation, and Stiffness Properties of Recycled Concrete Aggregate

Katarzyna Gabrys<sup>1,\*</sup>, Emil Soból<sup>2</sup> and Wojciech Sas<sup>1</sup>

<sup>1</sup> Water Centre WULS, Warsaw University of Life Sciences—WULS, 6 Ciszewskiego Street, 02-787 Warsaw, Poland; wojciech\_sas@sggw.edu.pl

<sup>2</sup> Department of Geotechnics, Warsaw University of Life Sciences—WULS, 159 Nowoursynowska Street, 02-787 Warsaw, Poland; emil\_sobol@sggw.edu.pl

\* Correspondence: katarzyna\_gabrys@sggw.edu.pl

**Abstract:** The construction sector is currently struggling with the reuse of waste originating from the demolition and modernization of buildings and roads. Furthermore, old buildings are gradually being replaced by new structures. This brings a significant increase of concrete debris to waste landfills. To prevent this, many studies on the possibilities of recycling concrete, known as recycled concrete aggregate (RCA), have been done. To broaden the applicability of reused concrete, an understanding of its properties and engineering behavior is required. A difficulty in sustainable, proper management of RCA is the shortage of appropriate test results necessary to assess its utility. For this reason, in the present study, the physical, deformation, and stiffness properties of RCA with gravely grain distribution were analyzed carefully in the geotechnical laboratory. To examine the mentioned properties, an extensive experimental program was planned, which included the following studies: granulometric analysis, Proctor and oedometer tests, as well as resonant column tests. The obtained research results show that RCA has lower values of deformation and stiffness parameters than natural aggregates. However, after applying in oedometer apparatus repetitive cycles of loading/unloading/reloading, some significant improvement in the values of the parameters studied was noticed, most likely due to susceptibility to static compaction. Moreover, some critical reduction in the range of linear response of RCA to dynamic loading was observed.

**Keywords:** anthropogenic material; laboratory tests; geotechnical properties



**Citation:** Gabrys, K.; Soból, E.; Sas, W. Physical, Deformation, and Stiffness Properties of Recycled Concrete Aggregate. *Sustainability* **2021**, *13*, 4245. <https://doi.org/10.3390/su13084245>

Academic Editor: José Ignacio Alvarez

Received: 1 March 2021

Accepted: 6 April 2021

Published: 11 April 2021

**Publisher's Note:** MDPI stays neutral with regard to jurisdictional claims in published maps and institutional affiliations.



**Copyright:** © 2021 by the authors. Licensee MDPI, Basel, Switzerland. This article is an open access article distributed under the terms and conditions of the Creative Commons Attribution (CC BY) license (<https://creativecommons.org/licenses/by/4.0/>).

## 1. Introduction

The development of a country's economy is very closely linked to the construction sector. On the one hand, this sector provides many jobs and uses building materials available on the market [1,2]. On the other hand, it becomes a producer of construction waste. The increasing costs of obtaining natural materials for earth construction in the form of debris and aggregates, in connection with the reduction of their resources and difficulties in obtaining them related to environmental protection, force us to apply waste materials.

There are many sources of waste materials. They come directly from the demolition of used construction objects, and they are generated as waste in the production of aggregates, in mining, energy, metallurgy, and chemical industries, while they can also be a form of municipal waste. The use of these materials in the civil engineering field requires recognition of both their technical properties and environmental risk, as well as the selection of appropriate embedding technology and quality control. Practical examples of the use of waste materials in the Polish construction sector, along with an assessment of their physical and mechanical parameters together with chemical composition are provided by Pisarczyk et al. [3] and Zabielska-Adamska [4]. Construction waste in the form of concrete debris that is recycled becomes recycled concrete aggregate (then called RCA). Recycling of concrete became not only a form of technical innovation but also a way to serve the needs

of modern urban society. RCA, after appropriate fractionation, can be successfully used in various civil engineering issues [5–7].

In recent years, RCA has become a promising and economical substitution for natural aggregates (NA) [8], finding extensive application in practical projects, including geotechnical and road engineering, as well as pavement construction [9]. Designers and constructors, however, are wary of using recycled aggregates, because their physical and mechanical properties are different from those characterizing NA [10]. Another critical topic is the lack of detailed knowledge about recycled aggregate properties [11]. Despite this, in the last four years, the demand for recycled aggregates increased from 5% to 8%, which is a significant increase on the scale of the European Union and EFTA (The European Free Trade Association) countries [11,12]. According to the data for 2015, published in the bulletins of the UEPG—European Aggregates Association [12], the most significant quantity of recycled aggregates is produced in the UK at 52.3 million tons, then in France at 20.3 million tons, while the quantity for Poland is 5 million tons.

The reuse of reclaimed concrete is essential from the sustainability point of view. Besides, recycled concrete is a material that can successfully merge economic and environmental interests. Research studies have shown that the reuse of materials reduces costs simultaneously on several levels: (a) by reducing the transport costs of waste materials, (b) by reducing the costs of removal and disposal, (c) by shortening the transport of materials for new buildings. It is expected that the price of RCA will decrease in the future, especially once the initial phase of development of production technology would be finished. At the same time, the price of NA should increase soon, as NA is less available, and in parallel, the transport cost will grow because sites will be further away. However, from an environmental point of view of the problem, the most important effect is still the reduction of pollution. Recycling is one aspect of waste management. With the introduction and development of quality control of waste management, we will see a pollution reduction very quickly over time [13].

This study aims to analyze the physical properties and mechanical behavior of RCA, as well as the response of RCA to dynamic stimuli, in terms of its possible use as a base and a subbase in road construction layers or embankment engineering structures, and other forms under static, dynamic, and cyclic loading caused mainly by the use of roads and rail transport. The problem of dynamic and cyclic loading is particularly important in the case of anthropogenic materials and soils due to the change in their properties as a result of man-made activity. RCA is a material with less recognized and, at the same time, more specific characteristics [14]. Nevertheless, in the scientific literature, a comparison of the above-mentioned RCA properties with the properties of natural aggregates can be found, as well as an analysis of the quantity and quality of recycled components used in various mixtures [15].

This paper is a contribution to a better understanding of RCA, a material that is problematic due to the large variability of its properties. Our research work focused on obtaining the stress and strain characteristics, as well as the characteristics of physical properties of RCA.

## 2. Materials and Methods

### 2.1. Material and Sample Preparation

The subject of research in the presented article is one type of anthropogenic soil, namely, Recycled Concrete Aggregate. In this study, RCA comes from the demolished buildings of the 1990s. Concrete aggregates were an element of concrete walls and floors, which strength class was estimated from C16/20 to C30/37, according to PN-EN 1992-1-1-2008 [16]. The strength class corresponds to concrete classes of C16/20—C30/37, following the standard PN-B-06250-1988 [17]. The material was mostly obtained from damaged concrete cubic samples with dimensions 150 × 150 × 150 mm. In 99% of cases, the aggregates were composed of broken cement concrete and less than 1% of glass and brick. After the crushing process, the resulting RCA did not contain impurities typical for

demolition material—steel, wood, and plastic (Figure 1). Glass elements and pieces of brick were also removed.

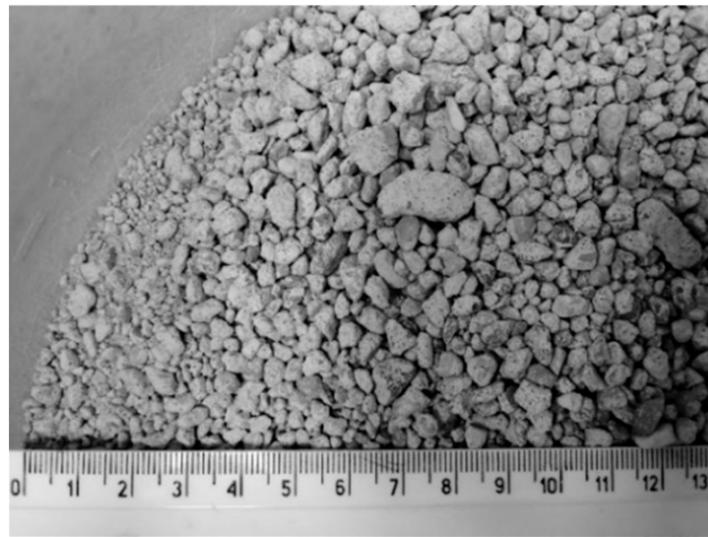


**Figure 1.** View of the fractured recycled concrete aggregate (RCA) without pieces of glass or brick.

To eliminate the influence of the secondary binding of RCA on its physical and mechanical properties, the material was seasoned in contact with water. Then, it was mixed to obtain a homogeneous structure, and, subsequently, it was fractioned with a mechanical shaker to the appropriate fractions, according to Galvín et al. [18]. Various mixtures with a granulometric composition corresponding to the particle size distribution curves used for road foundations based on the Polish technical standard [19] were created for further laboratory tests. In this paper, the results of one blend, i.e., 0–8 mm, are presented.

After the desired particle distribution was achieved, the water content of the mixture was determined using the Proctor method following PN-EN 13286-2:2010 [20]. The material was mixed with a suitable amount of water (about 9.5% of its net weight, based on the authors' previous research on this material [21]), allowing an optimum moisture content to be achieved.

As for sample preparation, for one-dimensional compression tests and dynamic tests, the previously prepared blend was compacted in an oedometer ring or a resonant column mold in five layers using Proctor's method [21]. The energy of compaction, at the optimum moisture content, was  $0.59 \text{ J}/\text{cm}^3$ . In one-dimensional compression tests, the samples with a diameter of 50 mm and a height of 20 mm were formed. For dynamic tests, the samples with  $d = 70 \text{ mm}$  and  $h = 140 \text{ mm}$  were created.

## 2.2. Physical Properties Analysis

To accurately characterize anthropogenic soil, it is necessary to determine its properties and applicability. For certain anthropogenic soils, their parameters differ from each other, so each time, it is crucial to check them precisely. All constructions using anthropogenic soils must be designed individually. The underlying physical and mechanical properties are:

- water content;
- grain size distribution analysis;
- bulk density, specific density;
- optimum moisture content and maximum bulk density of the soil skeleton;
- compressibility parameters;
- water permeability;
- California Bearing Ratio (CBR) CBR load index. The CBR is a measure of resistance of a material to penetration of a standard plunger under controlled density and moisture conditions.

For physical properties estimation, a series of various tests were conducted. Like the first one, the grain size analysis (sieve analysis) was performed. RCA, which is an alternative, granular material used in soil constructions, has a grain size distribution that allows classifying the mixtures as non-cohesive soil. The particle size curve of such materials is characterized by parameters describing the curvature and soil grain size, i.e.,  $C_U$ —coefficient of uniformity and  $C_C$ —coefficient of curvature [22,23].

The next stage of the study was to determine the compaction parameters of RCA. In practice, the Proctor impact method is used [24]. The test results from this method allow obtaining the optimum moisture content ( $w_{opt}$ ) and the maximum dry density ( $\rho_{d, max}$ ). They are the basis to carry out quality control of the implementation of soil structures, using the compaction index.

### 2.3. Deformation Properties Analysis

The deformation characteristics of soils include the consolidation indices ( $C_c$ ,  $C_s$ ,  $C_r$ ) and elastic moduli ( $E$ ,  $G$ ,  $K$ ,  $B$ ), as well as rate and creep parameters [25]. The research herein will focus on one-dimensional compression characteristics of recycled concrete aggregate using the oedometer test and next on elastic parameters, especially shear modulus, under dynamic loading using the resonant column test.

In the oedometer tests, a cylindrical RCA specimen was enclosed in a metal ring and subjected to a series of increasing static loads, while changes in thickness were recorded against time. From the changes in thickness at the end of each load stage, the compressibility of RCA was observed, and parameters measured such as the compression index ( $C_c$ ), recompression index ( $C_r$ ), and coefficient of volume compressibility ( $m_v$ ). From the changes in thickness recorded against time during a load stage, the rate of consolidation was recorded, and the coefficient of consolidation ( $c_v$ ) was measured.

The saturated specimen with a 50 mm diameter and 20 mm thick enclosed in a circular metal ring was sandwiched between porous stones. Vertical static load increments were applied at regular time intervals (e.g., 24 h). The load was doubled with each increment up to the required maximum (12.5, 25, 50, 100, 200, 400, 800, up to 1600 kPa). After full consolidation was reached, under the final load, the last loading step was removed up to 800 kPa. Afterward, the same specimen was reloaded (in two steps) up to a load of 3200 kPa, and it was allowed to swell. After the tests, the specimen was removed, and its thickness and water content were determined. In this study, one-dimensional consolidation tests on RCA samples were conducted under repetitive unloading and reloading conditions to investigate the compression behavior of the analyzed anthropogenic material.

### 2.4. Resonant Column Test Procedure

There exist many great techniques (in-situ and laboratory) from which stiffness parameters of soil can be derived [26,27]. As a part of the authors' research, several tests were carried out on the RCA properties under dynamic loading with the help of resonant frequency measurements. The laboratory tests were performed in Water Centre WULS, Poland, in the resonant column (RC) apparatus. A detailed description of this laboratory device can be found in Sas et al. [28].

In resonant column tests presented here, an axially confined cylindrical specimen (with dimensions: 70 mm diameter and 140 mm height) was vibrated employing torsional excitation of one of its ends. This allowed the sample's resonant frequency ( $f$ ) to be determined, which can be related to the device's stiffness using a theoretical elastic model. For RC tests, resonant frequency and acceleration determine the modulus and strain level [29]. Therefore, shear modulus ( $G$ ) and the maximum shear modulus (designated  $G_{MAX}$ ), or the small-strain shear modulus ( $G_0$ ) that provides an upper limit stiffness, were calculated from Equation (1):

$$G (G_{MAX}) = \rho_T V_S^2 = \rho_T \left( \frac{2\pi f l}{\beta} \right)^2, \quad (1)$$

where  $\rho_T$  is total mass density,  $V_S$  is shear wave velocity,  $f$  is the resonant frequency of RCA specimen,  $l$  is the specimen's length, and  $\beta$  stands for the parameter depends on a quotient of mass polar moment of inertia of soil specimen ( $I$ ) and mass polar moment of inertia of resonant column drive system ( $I_0$ ) [30]. The modulus  $G_{MAX}$  is a structural stiffness of all solids in civil engineering and can be measured in all soil types from colloids, clays, silts, sands, gravels, to boulders, and fractured rocks [25]. Interestingly,  $G_{MAX}$  applies to drained and undrained soil behavior, because at such small strains, pore water pressures have not yet been generated. Table 1 lists:

- the details of the resonant column tests program
  - a/ mean effective stress ( $p'$ ), corresponding to  $p' = \frac{\sigma'_1 + \sigma'_2 + \sigma'_3}{3}$ ,
  - b/ the output amplitude of the applied voltage,
- the details of the test material
  - a/ height ( $h$ ) and mass ( $m$ ) of the specimen,
  - b/ overconsolidation ratio (OCR), which can be computed from the preconsolidation stress ( $\sigma'_p$ ), and the overburden vertical effective stress ( $\sigma'_z$ ), as  $OCR = \frac{\sigma'_p}{\sigma'_z}$ ,
  - c/ bulk density ( $\rho$ ) is defined as the dry weight of soil per unit volume of soil, as  $\rho = \frac{m}{V}$ .

**Table 1.** Test conditions for resonant column tests.

Type of Loading	Mean Effective Stress	Output Amplitude	Height	Mass	Overconsolidation Ratio	Bulk Density
	$p'$ (kPa)	Range (V)	$h$ (mm)	$m$ (g)	OCR (-)	$\rho$ (g/cm <sup>3</sup> )
First loading	45	0.001–0.06	140.10	1056.33	1.0	1.96
	90	0.006–0.1	140.09	1029.38	1.0	1.91
	135	0.0005–0.07	139.95	1026.94	1.0	1.91
	180	0.0008–0.08	139.86	1009.94	1.0	1.88
	225	0.0004–0.08	139.81	986.46	1.0	1.83
Unloading	180	0.0005–0.08	139.82	982.20	1.25	1.83
	135	0.0005–0.06	139.84	985.65	1.67	1.83
	90	0.0005–0.06	139.87	996.87	2.5	1.85
	45	0.0005–0.02	139.82	1014.77	5.0	1.89
Reloading	90	0.0005–0.04	139.86	999.96	2.5	1.86
	135	0.0005–0.05	139.85	987.86	1.67	1.84
	180	0.0005–0.07	139.82	967.78	1.25	1.80
	225	0.0005–0.07	139.80	954.42	1.0	1.77
First loading	270	0.0005–0.07	139.76	937.07	1.0	1.74
	315	0.0005–0.1	139.73	889.42	1.0	1.65

### 3. Results and Discussion

#### 3.1. Physical Properties Results

Grain size distribution analysis was performed according to PKN-CEN ISO/TS 17892-4:2009 [31]. The results of the sieve analysis of the examined RCA are presented in Figure 2. This analysis led to the classification of the tested anthropogenic material as gravel with sand (saGr), according to Polish Committee for Standardization [32]. The distribution of particles from 0.06 mm to 10 mm is mostly in the range of the standard for aggregates used as improved sub-base and supporting other structures [19]. The values of the characteristic diameters ( $d_{10}$ ,  $d_{30}$ ,  $d_{50}$ ,  $d_{60}$ ) and coefficients ( $C_U$ ,  $C_C$ ), and typical characteristics for natural soils [32], are attached to Figure 2 as well. The obtained coefficient values:  $C_U = 9.09$  and  $C_C = 2.59$  classify our RCA as a well-graded material, susceptible to the compaction process, and suitable for earth constructions.

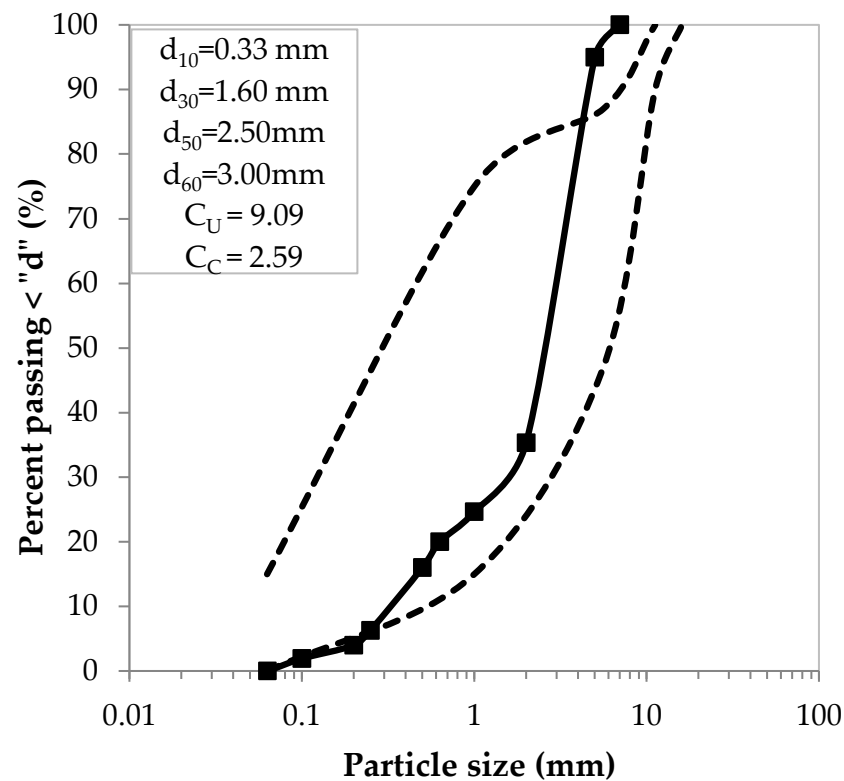


**Figure 2.** Result of the grain size analysis for the tested RCA—black line, upper and lower bound of optimal soil gradation curve by WT-4—black dotted line.

The optimum moisture content and maximum dry density were estimated with the Proctor method. The result of this test is shown in Figure 3. The maximum dry density ( $\rho_{d, \max}$ ) was equal to  $1.94 \text{ g/cm}^3$  and was achieved at the optimum moisture content ( $w_{\text{opt}}$ ) of about 9.5%. Very similar results to those are presented here, but for the blend of RCA from 0.05 to 2 mm can be found in Soból et al. [33]. Based on the results of compactability, it can be concluded that the tested RCA is compacted in a similar way to natural aggregates, where a characteristic value of the optimum moisture content is observed. The phenomenon of the strong linkage between  $w_{\text{opt}}$  with  $\rho_{d, \max}$ , and with the narrow range of moisture content noticeable in this study is a determinant of coarse-grained soils with a small percentage of fine particles content. This phenomenon is similar to the compaction of gravel with a low clay fraction [34]. Moreover, from Figure 3, it is also visible a dynamic increase of bulk density of the soil skeleton around  $w_{\text{opt}}$ , which is on the other hand characteristic for heterogeneous, multigrain material.

Other physical properties, such as water permeability and the CBR loading index, were examined in other authors' publications. The coefficient of permeability ( $k$ ) for the same RCA mixture was tested in Głuchowski et al. [14]. The results ranged from  $6.2 \times 10^{-6}$  to  $1.0 \times 10^{-5} \text{ m/s}$ , while the average value was  $2.1 \times 10^{-5} \text{ m/s}$ , which is similar to natural sandy and gravelly soils. The CBR loading is described by a percentage value, and for 0.06–8 mm RCA blend was from 71.7 to 101.5% for a 2.5-mm plunger depth and between 91.3 and 100.4% for 5.0-mm [20].

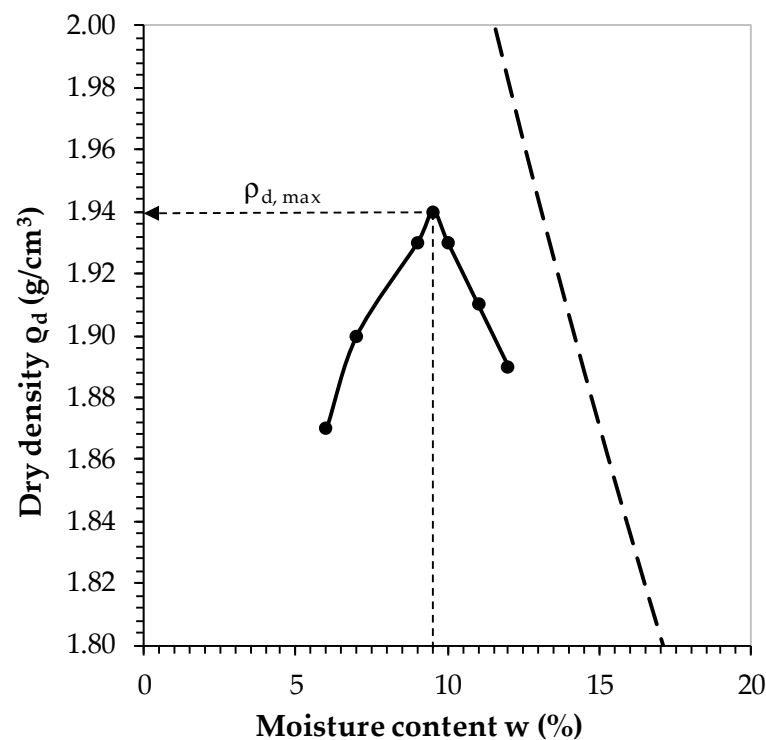


**Figure 3.** Result of the Proctor test for the tested RCA (black line: compaction curve, black dotted line—total saturation curve, theoretical maximum compaction).

### 3.2. Oedometer Tests Results

To measure the consolidation and compressibility parameters of our RCA, an oedometer test was employed. The saturated, compacted sample with 50 mm diameter and 20 mm thick had an initial volume density of 1.88 g/cm<sup>3</sup> and an initial void ratio of 0.554. At the end of the test (after loading of 3200 kPa), the specimen settled 1.278 mm, its volume density increased to 2.01 g/cm<sup>3</sup>, and its void ratio decreased to 0.455.

From the obtained results, two compressibility curves were drawn. The specimen height decreases with increasing stress on the arithmetic scale, which is presented in Figure 4. From this figure, three coefficients of volume compressibility ( $m_v$ ) and three oedometer compressibility modulus ( $M_0$ ,  $M$ ) were calculated in three stress ranges, namely: from 12.5 to 1600 kPa first loading, from 800 to 1600 reloading, and from 1600 to 3200 kPa first loading. In Figure 5, the relationship between void ratio and stress in the semi-logarithmic scale is presented. The compression index ( $C_C$ ) in the stress ranges from 12.5 to 1600 kPa and from 1600 to 3200 kPa, and the re-compression index ( $C_r$ ) in the stress range from 800 to 1600 kPa was calculated based on this figure. Moreover, from the consolidation curves for the stress values equal to 200, 400, 800, 1600, and 3200 kPa, a coefficient of consolidation ( $c_v$ ) was calculated.

In Table 2, the summary of parameters obtained from the oedometer test on RCA is presented. It can be seen that the oedometer modulus of primary loading ( $M_0$ ) has lower values than  $M_0$  for natural gravel soil. However, on the other hand, the oedometer modulus of secondary loading ( $M$ ) takes very high values. It can be connected with susceptibility to the crushing of recycled concrete aggregate. During the first loading process, grains of RCA are breaking under pressure, in particular cement mortar attached to natural aggregate. This leads to much higher settlements and, consequently, to lower values of  $M_0$ . Though, after the first crushing process, the specimen is statically compacted, and under the secondary loading process, only meager settlement occurs. This procedure can be observed based as well on the values of the other parameters, such as  $m_v$  or  $C_C$  and  $C_r$ . This phenomenon proves that RCA is highly susceptible to static compaction.

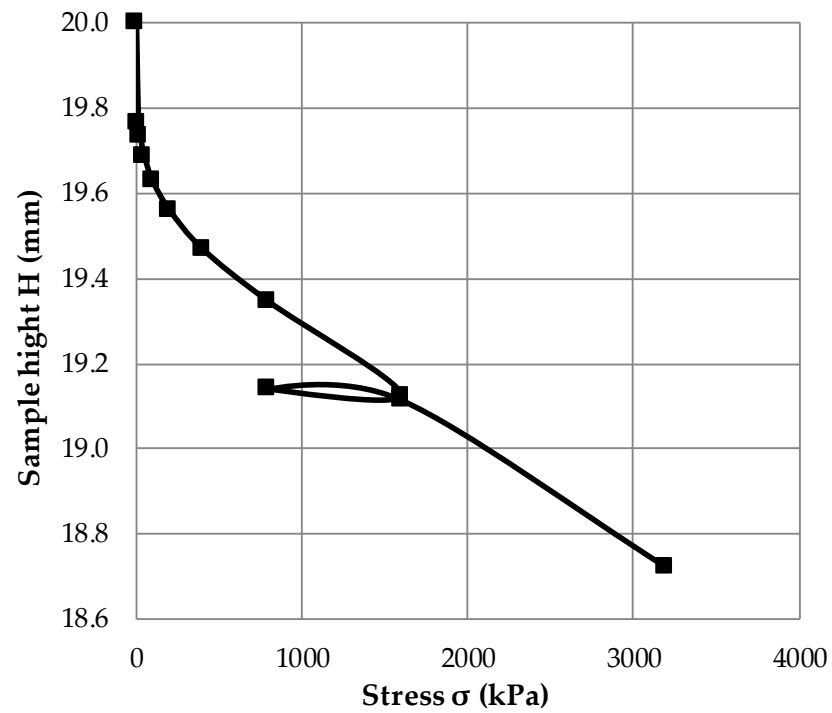


Figure 4. Compressibility curve of RCA from the oedometer test in arithmetic scale sample height depending on the stress.

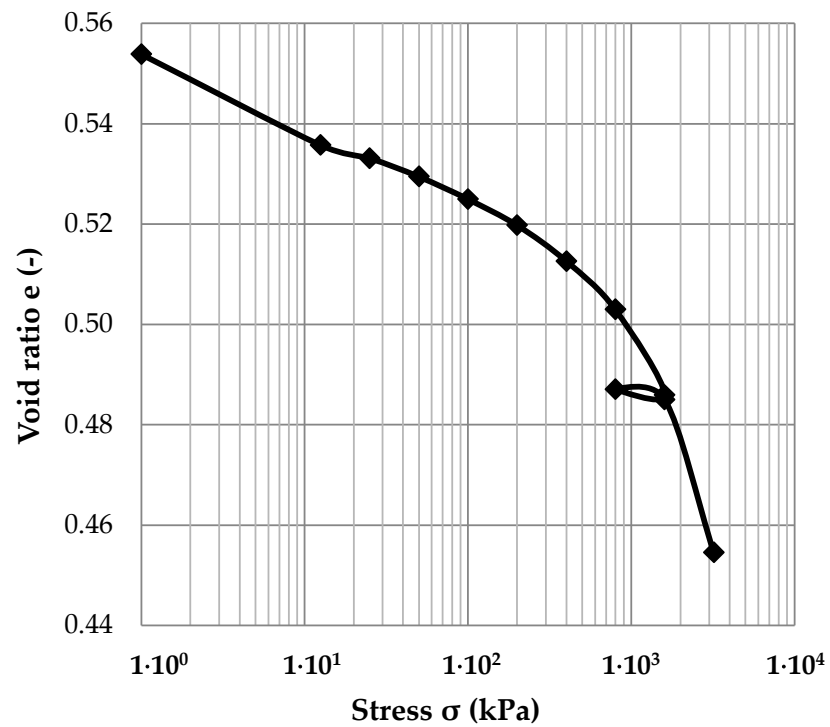


Figure 5. Compressibility curve of RCA from the oedometer test in a semi-logarithmic scale void ratio depending on the stress.

**Table 2.** Summary of parameters obtained from the oedometer test.

Parameter	Stress Range (kPa)				
	First Loading 12.5–1600		Reloading 800–1600		First Loading 1600–3200
Coefficient of volume compressibility $m_v$ (1/MPa)	0.0275		0.0017		0.0128
Oedometric modulus of primary loading $M_0$ (MPa)	36.33		-		78.02
Oedometric modulus of secondary loading $M$ (MPa)	-		588.92		-
Compression index $C_C$ (-)	0.024		-		0.101
Re—compression index $C_r$ (-)	-		0.0067		-
	Consolidation stress (kPa)				
	200	400	800 <sup>a</sup>	1600 <sup>a</sup>	3200
Coefficient of consolidation $c_v$ (m <sup>2</sup> /s)	0.003	0.005	0.004	0.003	0.0007
Average coefficient of consolidation $c_{v\text{ avg}}$ (m <sup>2</sup> /s)	0.003				

<sup>a</sup> First loading.

### 3.3. Dynamic Tests Results

During the resonant column test, shear modulus in small and medium strain ranges was measured, together with the degradation curve of this parameter. After the RCA specimen was created (Section 2.1), the anthropogenic material was saturated until Skempton's parameter equaled 0.95. Next, the consolidation stage and dynamic loading were carried out according to the schedule presented in Table 1.

In Figure 6, the degradation curves of the shear modulus of RCA for every consolidation stage are presented. It can be noticed that the values of  $G$  are from the range of 40 MPa at 45 kPa effective stress and 0.006% shear strain to 210 MPa at 315 kPa effective stress and 0.00006% shear strain. The shape of the curves coincides with those given in the literature, and it is similar to  $G$  degradation curves for natural gravel soil [35]. Moreover, the influence of stress history on shear modulus curves is visible in Figure 6. Namely, the curves obtained after the unloading process are above the results from the first loading and, consequently, the curves acquired in the second loading phase are above those obtained in the unloading process. This phenomenon is even more apparent in Figure 7, where  $G_{MAX}$  dependence on  $p'$  is presented. The values of  $G_{MAX}$  increase linearly with an increase in stress from 45 to 225 kPa (first loading phase). Next,  $G_{MAX}$  decreases linearly with a decrease in stress. However, for the same effective stress,  $G_{MAX}$  in the unloading stage has higher values than  $G_{MAX}$  from the first loading phase. Subsequently, when the next stage of the experiment is implemented and the mean effective stress increases again from 45 to 225 kPa, this results in higher values of  $G_{MAX}$  than in the unloading process. Thus, we can see an improvement in the stiffness parameter  $G$  after applying the loading, unloading, and reloading cycle. The same phenomenon was observed in He et al. [36]. It is worth noticing that an increase in stiffness from the reloading cycle is much more significant in our anthropogenic material than in natural sandy and gravely soil [36].

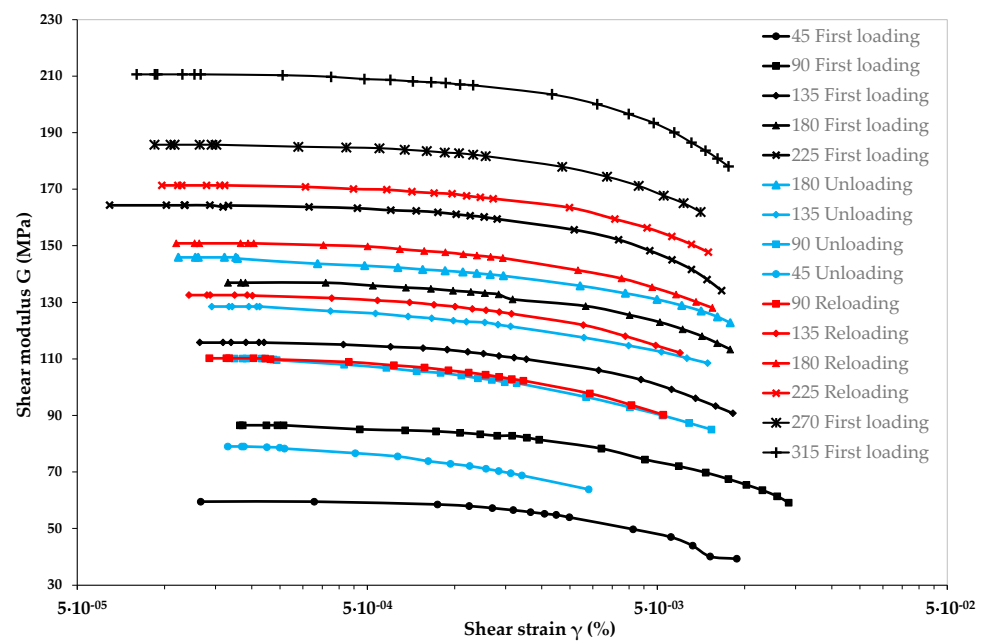


Figure 6. Degradation curves of shear modulus (G) of RCA obtained from resonant column tests.

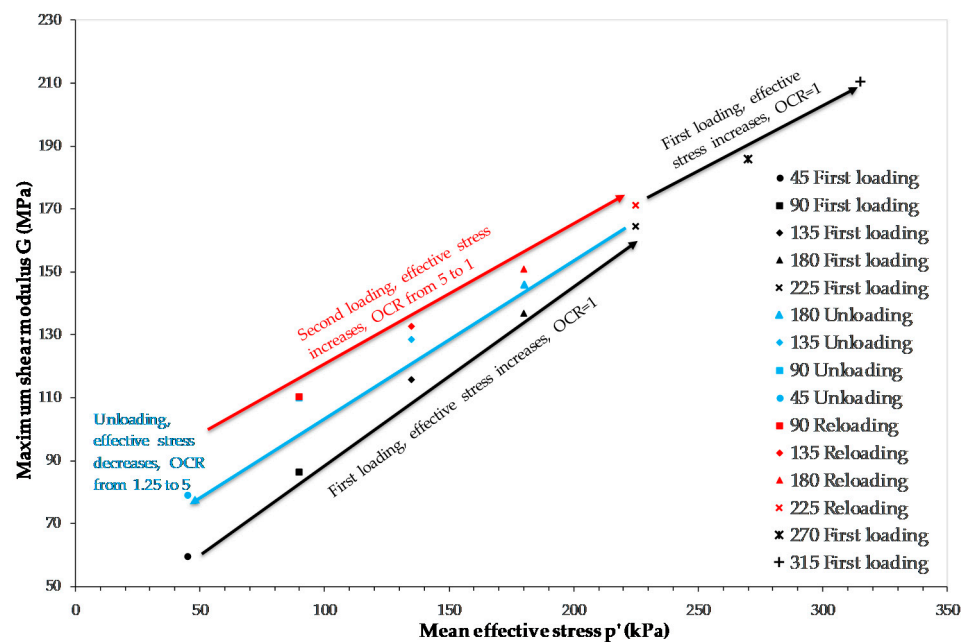


Figure 7. Maximum shear modulus ( $G_{MAX}$ ) of RCA depending on mean effective stress ( $p'$ ) and overconsolidation ratio (OCR).

In Figure 8, six normalized curves  $G/G_{MAX}$  are shown. These curves correlate with the smallest and largest stress values in a given phase of the experiment. Moreover, in Figure 8, the dashed horizontal line indicates the value of  $G/G_{MAX} = 0.98$ , which corresponds to the nonlinear threshold strain ( $\gamma_{tl}$ ) [37]. Nonlinear threshold strain is the border between two responses of a material subjected to dynamic loading. Before  $\gamma_{tl}$ , soil behaves like an elastic medium and has a linear response; after crossing  $\gamma_{tl}$ , the material's behavior is elasto-plastic, and its answer is nonlinear but still elastic.

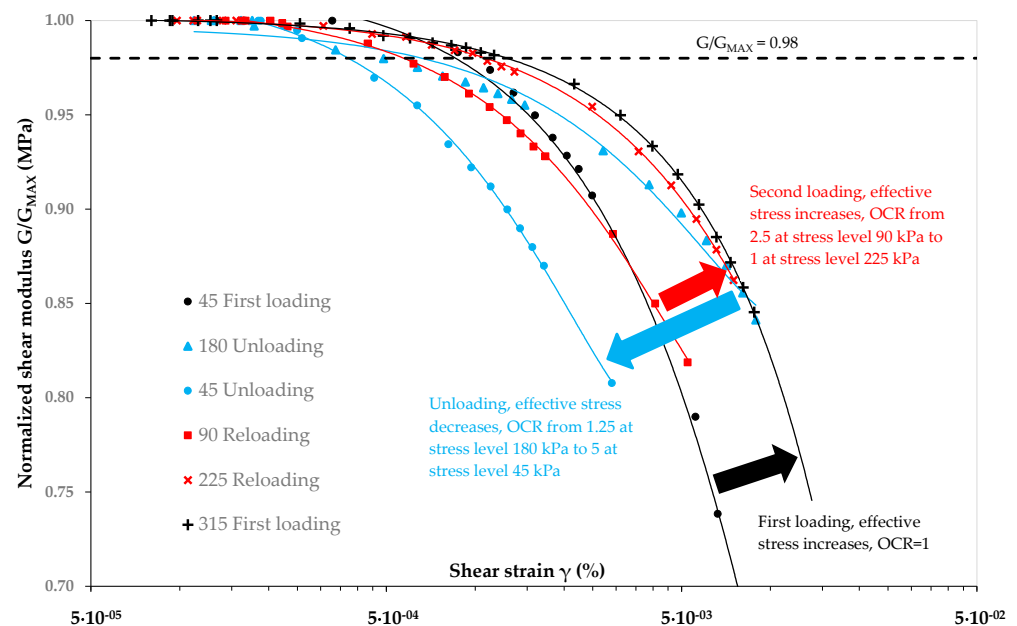


Figure 8. Normalized shear modulus  $G/G_{MAX}$  against shear strain  $\gamma$  of RCA.

The nonlinear threshold strain for RCA ranges from 0.00025% to 0.00066%, depending on the effective stress and experiment phase. Therefore, the linear RCA response increases with an increase in  $p'$  in the first loading stage. Then,  $\gamma_{tl}$  moves to a smaller strain along with the unloading process. Finally, the range of linear response of RCA increases again with the second loading stage. Generally, the most significant RCA linear response is for the first loading stage, and, on the other hand, the smallest range is for the unloading phase. Even after the second loading is completed,  $\gamma_{tl}$  is still lower than it was in the first loading. Thus, the loading/unloading/reloading cycle improves the stiffness parameter but, at the same time, reduces the range of linear response of RCA for dynamic loading. This occurrence may be related to high consolidation stress and micro-damage of RCA grains, in particular cement mortar attached to soil grains. They have lower compressive strength than natural soil grains. Consequently, micro-movements appear between grains, and the nonlinear threshold strain is achieved earlier.

#### 4. Conclusions

Recycled concrete aggregate is a relatively new construction material, whose applications can replace natural aggregates. To make it possible, extensive studies on its mechanical behavior and deformation characteristics are still necessary.

In the present paper, a series of various laboratory tests on recycled concrete aggregate were conducted. The results of this study lead to the following conclusions:

- The examined anthropogenic material is compacted in a similar way to natural aggregates, where a characteristic value of the optimum moisture content is observed. The tested RCA achieved maximum dry density  $\rho_{d, max} = 1.94 \text{ g/cm}^3$  at the optimum moisture content of 9.5%.
- Oedometric modulus of primary loading ( $M_0$ ) had lower values than for natural aggregates. However, the oedometric modulus of secondary loading ( $M$ ) had an extremely high value. Such results are connected with the susceptibility of RCA on static compaction. Other deformation parameters obtained from the oedometer test behaved in the same manner.
- Shear modulus degradation curves of RCA had the same shape as the same curves but for natural aggregates.
- Due to the loading/unloading/reloading cycle, some improvement in  $G_{MAX}$  values was observed. Stress history had a more significant impact on stiffness properties in

RCA than in natural gravel soil, which results again from the susceptibility of RCA on static compaction.

- Due to the loading/unloading/reloading cycle, a significant reduction of the range of linear response of RCA for dynamic loading is observed. This can be related to high consolidation stress values and micro-damage of RCA grains.
- Extensive studies should still be conducted on the crushing properties of RCA, as well as on the impact of this process on various geotechnical parameters, like hydraulic conductivity, effective stress, consolidation, and shear strength parameters.

**Author Contributions:** Conceptualization, K.G. and E.S.; methodology, K.G.; validation, W.S.; formal analysis, K.G. and E.S.; investigation, E.S.; resources, W.S.; data curation, E.S.; writing—original draft preparation, K.G.; writing—review and editing, K.G.; visualization, E.S.; supervision, W.S.; project administration, W.S. All authors have read and agreed to the published version of the manuscript.

**Funding:** This research received no external funding.

**Institutional Review Board Statement:** Not applicable.

**Informed Consent Statement:** Not applicable.

**Data Availability Statement:** Data available on request due to their size properties. The data presented in this study are available on request from the corresponding author.

**Conflicts of Interest:** The authors declare no conflict of interest.

## References

1. Skotnicki, Ł.; Kuźniewski, J. Zastosowanie kruszywa betonowego z recyklingu w mieszankach mineralno-cementowo-emulsyjnych. *Przegląd Komun.* **2018**, *11*, 30–36.
2. Sas, W.; Głuchowski, A.; Szymański, A. Behavior of recycled concrete aggregate improved with lime addition during cyclic loading. *Int. J. Geomate* **2016**, *10*, 1662–1669. [[CrossRef](#)]
3. Pisarczyk, S.; Falaciński, P.; Żuraw, L. Wykorzystanie odpadów budowlanych w inżynierskich konstrukcjach ziemnych. *Pr. Nauk. Politech. Warszawskiej. Inżynieria Sr.* **2003**, *45*, 5–25.
4. Zabielska-Adamska, K. Wybrane zastosowania materiałów odpadowych w Geoinżynierii. *Inżynieria Morska Geotech.* **2012**, *4*, 286–293.
5. Kijowski, G. Kruszywo z betonu. *Bud. Technol. Archit.* **2006**, *2*, 46–47.
6. Rafalski, L. *Podbudowy Drogowe*; IBDiM, Ed.; IBDiM: Warszawa, Poland, 2007. [[CrossRef](#)]
7. Sas, W.; Szymański, A.; Malinowska, E.; Gabryś, K. Geotechniczne uwarunkowania zastosowania materiałów antropogenicznych w budownictwie. *Inżynieria Morska Geotech.* **2012**, *4*, 376–389.
8. He, H.; Senetakis, K.; Coop, M.R. Stiffness of recycled composite aggregate. *Soil Dyn. Earthq. Eng.* **2018**, *110*, 185–194. [[CrossRef](#)]
9. Tatsuoka, F.; Tomita, Y.I.; Iguchi, Y.; Hirakawa, D. Strength, and stiffness of compacted crushed concrete aggregate. *Soils Found* **2013**, *53*, 835–852. [[CrossRef](#)]
10. Głuchowski, A.; Gabryś, K.; Soból, E.; Šadzevičius, R.; Sas, W. Geotechnical properties of anthropogenic soils in road engineering. *Sustainability* **2020**, *12*, 4843. [[CrossRef](#)]
11. Cardoso, R.; Silva, R.V.; de Brito, J.; Dhir, R. Use of recycled aggregates from construction and demolition waste in geotechnical applications: A literature review. *Waste Manag.* **2016**, *49*, 131–145. [[CrossRef](#)]
12. UEPG. *A Sustainable Industry for a Sustainable Europe*; Annual Review, UEPG: Brussels, Belgium, 2017.
13. Curović, N. Recycled concrete—ecology and economic criterias. *J. Appl. Eng. Sci.* **2016**, *14*, 271–274. [[CrossRef](#)]
14. Głuchowski, A.; Sas, W.; Dziecioł, J.; Soból, E.; Szymański, A. Permeability and Leaching Properties of Recycled Concrete Aggregate as an Emerging Material in Civil Engineering. *Appl. Sci.* **2019**, *9*, 81. [[CrossRef](#)]
15. Lima, C.; Caggiano, A.; Faella, C.; Martinelli, E.; Pepe, M.; Realfonzo, R. Physical properties and mechanical behavior of concrete made with recycled aggregates and fly ash. *Constr. Build. Mater.* **2013**, *47*, 547–559. [[CrossRef](#)]
16. PN-EN 1992-1-1-2008. Eurokod 2. Projektowanie konstrukcji z beton. Część 1-1: Reguły ogólne i reguły dla budynków. Available online: <https://sklep.pkn.pl/pn-en-1992-1-1-2008p.html> (accessed on 14 March 2008).
17. PN-B-06250-1988. Beton zwykły. Available online: <https://docer.pl/doc/s8v5n15> (accessed on 14 March 2008).
18. Galvín, A.P.; Ayuso, J.; García, I.; Jiménez, J.R.; Gutiérrez, F. The effect of compaction on the leaching and pollutant emission time of recycled aggregates from construction and demolition waste. *J. Clean. Prod.* **2014**, *83*, 294–304. [[CrossRef](#)]
19. WT-4:2010. Załącznik Nr 3 do Zarządzenia nr 102 Generalnego Dyrektora Dróg Krajowych i Autostrad z dnia 19 Listopada 2010 r.: Mieszanki Niezwiązane do dróg Krajowych WT-4 2010 Wymagania Techniczne, Warsaw, Poland. Available online: [https://www.gddkia.gov.pl/userfiles/articles/d/Dokumenty\\_techniczne/WT4.pdf](https://www.gddkia.gov.pl/userfiles/articles/d/Dokumenty_techniczne/WT4.pdf) (accessed on 18 April 2010).

20. PN-EN 13286-2:2010. Mieszanki Niezwiązane i Związane Spoiwem Hydraulicznym. Część 2: Metody Określania Gęstości i Zawartości Wody. Zagęszczanie metodą Proctora. Available online: <https://sklep.pkn.pl/pn-en-13286-2-2010e.html> (accessed on 31 July 2009).
21. Sas, W.; Głuchowski, A.; Gabryś, K.; Soból, E.; Szymański, A. Deformation Behavior of Recycled Concrete Aggregate during Cyclic and Dynamic Loading Laboratory Tests. *Materials* **2016**, *9*, 780. [[CrossRef](#)] [[PubMed](#)]
22. Gabryś, K.; Sas, W.; Soból, E.; Głuchowski, A. Torsional shear device for testing the dynamic properties of recycled material. *Studia Geotech. Mech.* **2016**, *38*, 15–24. [[CrossRef](#)]
23. Gabryś, K.; Soból, E.; Sas, W.; Šadzevičius, R.; Skominas, R. Warsaw Glacial Quartz Sand with different grain-size characteristics and its shear wave velocity from various interpretation methods of BET. *Materials* **2021**, *14*, 544. [[CrossRef](#)]
24. Bowles, J.E. *Engineering Properties of Soils and Their Measurement*, 4th ed.; McGraw-Hill: New York, NY, USA, 2001.
25. Mayne, P.W. Stress-Strain-Strength-Flow Parameters from Enhanced in-Situ Tests. In Proceedings of the International Conference on In-Situ Measurement of Soil Properties & Case Histories In-Situ, Bali, Indonesia, 21–24 May 2001; pp. 27–48.
26. Clayton, C.R.I. Stiffness at small strain: Research and practice. *Géotechnique* **2011**, *61*, 5–37. [[CrossRef](#)]
27. Huang, X.; Zhou, A.; Wang, W.; Jiang, P. Characterization of the dynamic properties of clay-gravel mixtures at low strain level. *Sustainability* **2020**, *12*, 1616. [[CrossRef](#)]
28. Sas, W.; Gabryś, K.; Szymański, A. Experimental studies of dynamic properties of Quaternary clayey soils. *Soil Dyn. Earthq. Eng.* **2017**, *95*, 29–39. [[CrossRef](#)]
29. Gabryś, K.; Soból, E.; Markowska-Lech, K.; Szymański, A. *Shear Modulus of Compacted Sandy Clay from Various Laboratory Methods*; (IOP Conference Series Materials Science and Engineering 471 4); IOP Publishing: Bristol, UK, 2019; p. 042022.
30. GDS Instruments Ltd. *2010 Product Helpsheets*; GDS Instruments Ltd.: Hook, UK, 2010.
31. PN-EN ISO 17892-4:2017-01 Rozpoznanie i badania geotechniczne—Badania laboratoryjne gruntów—Część 4: Badanie uziarnienia gruntów. Available online: <https://sklep.pkn.pl/pn-en-iso-17892-4-2017-01e.html> (accessed on 22 February 2018).
32. PN-EN ISO 14688-1: 2018-05 Rozpoznanie i badania geotechniczne—Oznaczenie i klasyfikowanie gruntów—Część 1: Oznaczenie i opis. Available online: <https://sklep.pkn.pl/pn-en-iso-14688-1-2018-05e.html> (accessed on 22 February 2018).
33. Soból, E.; Sas, W.; Szymański, A. Scale effect in direct shear tests on recycled concrete aggregate. *Studia Geotech. Mech.* **2016**, *37*, 45–49. [[CrossRef](#)]
34. Wolski, W.; Król, P.; Sas, W. *Les Problèmes D'utilisation des Gravier Argileus Humides. De Bonne Granulometries, pour les Recharges des Barrages en Terre*; XVII congress ICOLD: Paris, France, 1991; Volume 67.
35. Bayat, M.; Ghalandarzadeh, A. Stiffness degradation and damping ratio of sand-gravel mixtures under saturated state. *Int. J. Civ. Eng.* **2018**, *16*, 1261–1277. [[CrossRef](#)]
36. He, H.; Payan, M.; Senetakis, K. The behavior of a recycled road base aggregate and quartz sand with bender/extender element tests under variable stress state. *Eur. J. Environ. Civ. Eng.* **2018**, 1–18. [[CrossRef](#)]
37. Vucetic, M. Cyclic threshold shear strains in soils. *J. Geotech. Eng.* **1994**, *120*, 2208–2228. [[CrossRef](#)]